Interface Focus

Interface Focus (2012) **2**, 292–306
doi:10.1098/rsfs.2011.0121
Published online 21 March 2012

Review

Mesoporous bioactive glasses: structure characteristics, drug/growth factor delivery and bone regeneration application

Chengtie Wu and Jiang Chang*

State Key Laboratory of High Performance Ceramics and Superfine Microstructure, Shanghai Institute of Ceramics, Chinese Academy of Sciences, Shanghai 200050, People's Republic of China

The impact of bone diseases and trauma in the whole world has increased significantly in the past decades. Bioactive glasses are regarded as an important bone regeneration material owing to their generally excellent osteoconductivity and osteostimulativity. A new class of bioactive glass, referred to as mesoporous bioglass (MBG), was developed 7 years ago, which possess a highly ordered mesoporous channel structure and a highly specific surface area. The study of MBG for drug/growth factor delivery and bone tissue engineering has grown significantly in the past several years. In this article, we review the recent advances of MBG materials, including the preparation of different forms of MBG, composition–structure relationship, efficient drug/growth factor delivery and bone tissue engineering application. By summarizing our recent research, the interaction of MBG scaffolds with bone-forming cells, the effect of drug/growth factor delivery on proliferation and differentiation of tissue cells and the *in vivo* osteogenesis of MBG scaffolds are highlighted. The advantages and limitations of MBG for drug delivery and bone tissue engineering have been compared with microsize bioactive glasses and nanosize bioactive glasses. The future perspective of MBG is discussed for bone regeneration application by combining drug delivery with bone tissue engineering and investigating the *in vivo* osteogenesis mechanism in large animal models.

Keywords: mesoporous bioglass scaffolds; drug/growth factor delivery; bone tissue engineering; osteogenesis; bioactivity

1. THE RATIONALE FOR DESIGNING AND DEVELOPING MESOPOROUS BIOGLASS

1.1. Conventional bioactive glasses

Bioactive glasses have played an increasingly important role in bone tissue regeneration application by virtue of their generally excellent osteoconductivity, osteostimulation and degradation rate [1–6]. Typically, the melt bioactive glass, called 45S5 bioglass, was pioneered by Hench [7,8] and was first developed using the traditional melt method at high temperatures (1300–1500°C). The 45S5 bioglass has been regarded as a bioactive bone regeneration material that is able to bond closely with the host bone tissue [7]. The mechanism behind new bone formation on bioactive glass is closely associated with the release of Na^+ and Ca^{2+} ions and the deposition of a carbonated hydroxyapatite (CHAp) layer. The apatite layer forms a strong chemical bond between 45S5 bioglass and host bone [7]. Further studies have also shown that the Ca- and Si-containing ionic products released from the 45S5 contribute to its bioactivity, as both Ca and Si are found to stimulate osteoblast proliferation and differentiation [9–13]. Xynos *et al.* further found that 45S5 bioglass is able to enhance the expression of a potent osteoblast mitogenic growth factor, insulin-like growth factor II (IGF-II) [12,14]. The 45S5 bioglass is still considered to be the gold standard for bioactive glasses, although melt bioactive glass has a number of limitations [14]. One of these limitations is that it needs to be melted at a very high temperature (greater than 1300°C), and the other is its lack of microporous structure inside the materials with a low specific surface area; therefore, the bioactivity of melt bioactive glasses will mainly depend on the content of SiO_2 [14]. Generally, the bioactivity of melt bioactive glasses will decrease with an increase in SiO_2

*Author for correspondence (jchang@mail.sic.ac.cn).

One contribution of 11 to a Theme Issue 'Biomaterials research in China'.

Received 5 December 2011
Accepted 27 February 2012

content [2,8,15]. When the SiO_2 content exceeds 60 per cent, the bioactive glass is not able to induce a CHAp layer even after several weeks in simulated body fluid (SBF) and fails to bond to either bone or soft tissues [16]. The main reason is that high SiO_2-containing glasses prepared by the melt method have a stable net structure and therefore cannot easily release Na^+ and Ca^{2+} ions, leading to insufficient OH^- groups on the surface of glasses to induce apatite formation.

Besides silicate glasses, phosphate glasses have been studied for bone regeneration application. Knowles and co-workers [17] suggested that although silica-based bioglasses could form a direct bond with the surrounding bone tissue and were clinically approved for bone repair applications, the compositional range of these glasses was limited. Alternatively, phosphate-based glasses, which are similar to the inorganic component of bone, have the unique property that their degradation can be adjusted to vary from a few hours to several weeks by incorporating different oxides according to the end application [17–19]. Phosphate bioceramics, hydroxyapatite (HAp) ceramics, are widely used for bone tissue replacement and regeneration owing to their generally good biocompatibility and similar chemical composition with biological apatite in bone tissues. However, sintered stoichiometric HAp ceramics have a limited ability to form an interface with, and to stimulate the development of new bone tissue [20,21]. Also, the sintered HAp does not degrade significantly but rather remains as a permanent fixture susceptible to long-term failure [22]. Previously, ion (e.g. Mg)-doped HAp was developed to improve their biological response [23]. Compared with HAp ceramics, bioactive glasses seem to have better *in vitro* bioactivity and quicker degradation [7].

In the early 1990s, in an effort to overcome the limitation of melt bioactive glasses, Li *et al.* [24] prepared sol–gel bioactive glasses. They demonstrated that this class of materials was bioactive in a wider compositional range when compared with the traditional melt bioglass. The glasses in the SiO_2–CaO–P_2O_5 system had SiO_2 contents of up to 90 per cent and were still capable of inducing the formation of apatite layers, compared with the 60 per cent SiO_2 boundary of the melt bioactive glasses [25]. Owing to its greater surface area and porosity—properties from the sol–gel process—the range of bioactive compositions for sol–gel bioglass is wider, and when compared with melt bioactive glasses, these bioactive glasses exhibit higher bone bonding rates coupled with excellent degradation and resorption properties [16,26,27]. Although sol–gel bioactive glasses have a better composition range and bioactivity than melt bioactive glasses, the micropore distribution is not uniform and inadequate for efficient drug loading and release [14,28].

1.2. Mesoporous SiO_2 materials

In the past 20 years, mesoporous materials have attracted great attention owing to their significant features of a large surface area, ordered mesoporous structure, tunable pore size and volume, and well-defined surface property. They have many potential applications, such as catalysis, adsorption/separation, biomedicine, etc. [29]. The studies of the applications of mesoporous materials have been expanded into the field of biomaterial science for drug delivery and bone regeneration application. Vallet-Regí and co-workers [30–32] systematically investigated the *in vitro* apatite formation of different types of mesoporous SiO_2 materials, and they demonstrated that an apatite-like layer can form on the surfaces of Mobil composition of matter (MCM)-48, hexagonal mesoporous silica (SBA-15), phosphorus-doped MCM-41, and bioglass-containing MCM-41, allowing their use in biomedical engineering for tissue regeneration. Mesoporous silica (SiO_2) was also used for the study of efficient drug delivery. It is found that mesoporous silica is an attractive material owing to its good biocompatibility, low cytotoxicity, tailored surface charge and enormous possibilities for organic functionalization [32–34]. In addition, mesoporous silica presents unique mesopore structures and porosities with a large surface area, high pore volume and narrow mesopore channels, which allow the adsorption of drugs and biomelecules into their well-ordered system of pores and cavities to be then locally released [33]. However, although pure mesopore silica has been shown to be a potential drug-delivery system, it has generally too low an activity of *in vitro* apatite mineralization to be considered for bioactive bone grafts [35,36].

1.3. Why develop mesoporous bioglass materials?

In bone reconstruction surgeries, osteomyelitis caused by bacteria infection is the main complication. Conventional treatments include systemic antibiotic administration, surgical debridement, wound drainage and implant removal [37]. These approaches, however, are not always efficient, and the patients may suffer from extra surgeries. An alternative approach to solve the problem is to introduce a local drug release system into the implant site [38]. The advantages of this treatment include high delivery efficiency, continuous action, reduced toxicity and convenience to the patients [37,39]. Therefore, to overcome the limitations of conventional bioactive glasses (without well-ordered mesopore structures for drug delivery) and pure mesopore SiO_2 (low bioactivity), it is of great importance to design and develop a new class of biomaterials that combine efficient drug delivery and excellent bioactivity. The concept has been previously developed by Vallet-Regi (as shown in figure 1) [40]. Yu and co-workers [41,42], for the first time, prepared mesoporous bioglasses (MBGs) in 2004 by the combination of the sol–gel method and the supramolecular chemistry of surfactants. Their study has opened a new direction for applying nanotechniques to regenerative medicine by coupling drug delivery with bioactive materials. These materials are based on a CaO–SiO_2–P_2O_5 composition and have a highly ordered mesopore channel structure, with a pore size ranging from 5 to 20 nm. Compared with conventional non-mesoporous bioactive glasses (NBGs), the MBGs possess a more optimal surface area, pore volume, ability to induce *in vitro* apatite

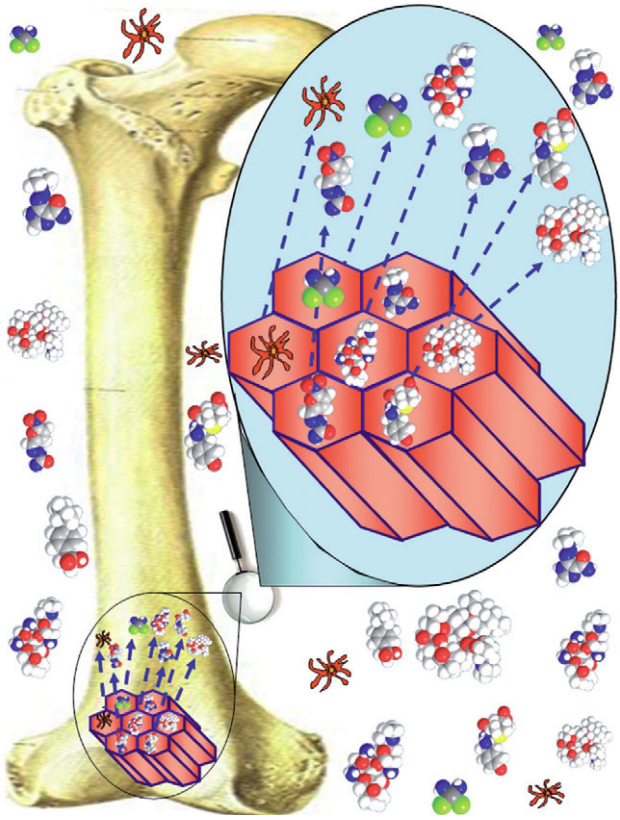

Figure 1. The concept of MBG for drug delivery and bone regeneration [40].

mineralization in SBF and excellent cytocompatibility [42–45]. The study of MBG for drug delivery and bone tissue engineering has been a hot area of research over the past 5 years. In this article, we review the recent advances for the different forms of MBG materials. By summarizing the research progress in our group, the interaction of three-dimensional MBG scaffolds with bone-forming cells, the effect of drug/growth factor delivery on the function of tissue cells and the *in vivo* osteogenesis of MBG scaffolds are mainly highlighted.

2. PREPARATION METHODS AND MESOPORE STRUCTURE CHARACTERISTICS OF MESOPOROUS BIOGLASS

2.1. Mesopore formation and selection of structure-directing agents for mesoporous bioglass

The preparation of MBG is similar to that for mesoporous SiO_2, in which the supramolecular chemistry has been incorporated into the sol–gel process. In this strategy, the incorporation of structure-directing agents (e.g. cetyltrimethyl ammonium bromide (CTAB), P123 and F127) is essential for obtaining well-ordered structures. Under appropriated synthesis conditions, these molecules self-organize into micelles. Micelles link the hydrolysed silica precursors through the hydrophilic component and self-assemble to form an ordered mesophase [16,28]. Then the mixture reaction system of bioactive glasses and structure-directing agents undergoes an evaporation-induced self-assembly (EISA) process. A general definition of EISA is the spontaneous organization of materials through non-covalent interactions (hydrogen bonding, van der Waals forces, electrostatic forces, etc.) with no external intervention [46]. In the EISA process of MBG, the surfactants assemble into micelles, spherical or cylindrical structures that maintain the hydrophilic parts of the surfactants in contact with the composition of bioactive glasses (Si, Ca and P elements, etc.) while shielding the hydrophobic parts within the micellar interior. Once the mixture is dried and the surfactant removed, a well-ordered mesoporous structure will be obtained, exhibiting high surface area and porosity [16].

Currently, the structure-directing agents for preparing MBG mainly include CTAB, F127 (EO106-PO70-EO106) and P123 (EO20-PO70-EO20). It is found that the structure-directing agents play an important role in influencing the mesopore structure, mesopore size, surface area and pore volume of MBG. Generally, CTAB-induced MBG had a smaller mesopore size (2–3 nm) than P123- or F127-derived MBG (4–10 nm). P123 induced a two-dimensional hexagonal (p6mm) mesopore structure. F127 induced a wormlike mesopore structure [41]. Our study has found that the orderings of the mesopores in CTAB-induced MBG materials are lower than that of P123- or F127-induced MBG materials (figure 2). The effect of structure-directing agents on the textural characteristics of MBG is shown in table 1. By comparing the preparation methods of applying different structure-directing agents, generally, the usage of P123 and F127 to prepare MBG is much easier than that of CTAB. The usage of CTAB needs additional procedures to filter and wash the obtained materials prior to calcining, but the methods of P123 and F127 do not need these procedures.

2.2. The methods to prepare different forms of current mesoporous bioglass: particles, fibres, scaffolds and composites

MBG has been prepared as particles [41], fibres [61], spheres [62], three-dimensional scaffolds [63] and composites with well-ordered mesoporous channel structure and excellent bioactivity for drug delivery and bone regeneration application. Since current MBG materials have different forms, their preparation methods are significantly different. Generally, all forms of MBG materials require the usage of structure-directing agents to form a mesoporous structure, and by combining other preparation techniques, different forms of MBG can be obtained.

The preparatory method of MBG particles by simply using structure-directing agents is much easier than other methods of preparation of MBG materials. MBG particles were firstly synthesized in 2004 [41]. The size of the obtained MBG particles is around several tens of micrometres. The particles contain highly ordered mesoporous channels (5 nm) with a highly specific surface area and pore volume. After that, Lei *et al.* [64] synthesized MBG powders with a highly specific surface area by using acetic acid as a structure-assisting

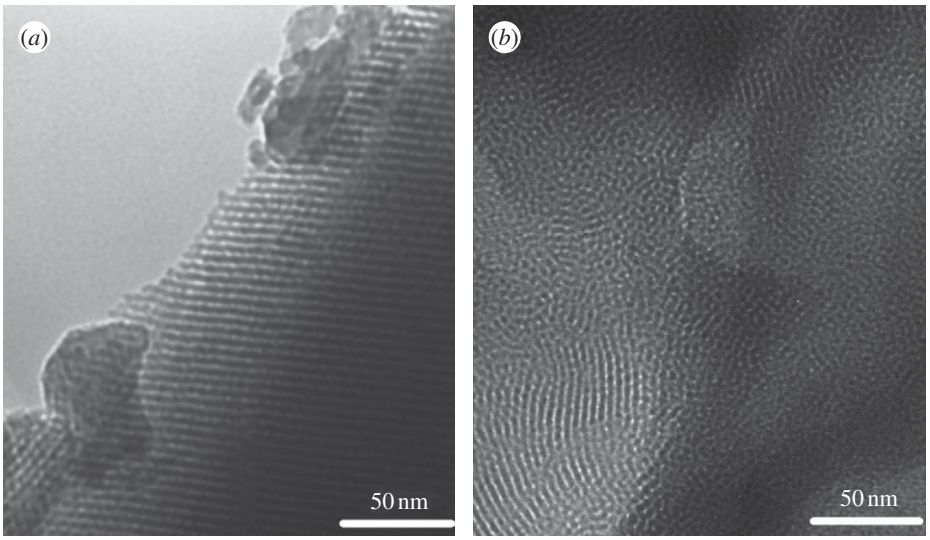

Figure 2. Transmission electron microscopy images of (*a*) P123-induced MBG and (*b*) CTAB-induced MBG. P123 induced a more ordered mesopore structure than CTAB.

Table 1. The textural characteristics of MBG prepared by different structure-directing agents. P123, $EO_{20}PO_{70}EO_{20}$; F127, $EO_{106}PO_{70}EO_{106}$; F108, $EO_{132}PO_{70}EO_{132}$; B50-6600, $EO_{39}BO_{47}EO_{39}$; P85, $EO_{26}PO_{39}EO_{26}$; CTAB, cetyltrimethyl ammonium bromide.

structure-directing agents	surface area ($m^2\,g^{-1}$)	pore volume ($cm^3\,g^{-1}$)	pore size (nm)	references
P123	300–350	0.4–0.49	4.3–4.6	[41]
	278–400	0.54–0.73	6.5–6.9	[47]
	250–350	0.4–0.5	5	[48–51]
	438–466		3.5–3.7	[52]
	450–480	0.63–0.73	5.37–6.43	[44]
	499	0.7	6.1	[53]
F127	520	0.51	5.4	[54]
	228–300	0.36–0.42	5.0–7.1	[41]
	152–310	0.235–0.356	4.2–5.0	[55]
F108	516		5	[56]
B50-6600	301	0.41	6.4	[57]
P85	328	0.36	3.4	[57]
CTAB	1040	1.54	1.82–2.2	[58]
	443	0.57	2.9	[59]
P123 + CTAB	552–618	0.69–1.08	4.1–6.2	[60]

agent and hydrolysis catalyst. MBG powders with different compositions (58S and 77S) were prepared by using P123 and hydrothermal treatment, both of which were shown to have excellent *in vitro* bioactivity [47,65]. By using the same method, Li *et al.* [66] prepared Mg-, Zn- or Cu-containing multicomponent MBG particles. Wu *et al.* [52] synthesized $CaO–SiO_2$ mesoporous MBG particles for haemostatic applications. Recently, our group developed a simple method to prepare MBG particles without hydrothermal treatment, which is suitable for large-mass production of MBG particles [67].

MBG fibres were prepared by a combination of structure-directing agents and electron spin techniques. Hong *et al.* prepared ultrathin MBG fibres by electron spin techniques [61]. In their study, ultrathin MBG fibres, with hierarchical nanoporosities and high matrix homogeneities, were synthesized using the electrospinning technique and P123–PEO co-templates [61]. At the same time, by controlling the electrospinning conditions, they were able to prepare MBG fibres with hollow cores and mesoporous walls; these fibres were found to be highly bioactive for drug delivery [14,68].

MBG spheres could be prepared by a combination of structure-directing agents and other special techniques, such as alginate cross-linking, co-templates and hydrothermal methods. We recently developed a millimetre-sized MBG sphere by using the method of alginate cross-linking with Ca^{2+} ions. The large-size MBG spheres could not only support the adhesion of bone marrow stromal cells (BMSCs), but also control the delivery of proteins [62]. Yun *et al.* [56] prepared hierachical mesoporous–macroporous MBG spheres with a size of several hundred micrometres in a hydrophobic solvent (chloroform) by the triblock copolymer templating and sol–gel technique. The spheres have well-interconnected pore structures and excellent *in vitro* bioactivity. Mesoporous hollow bioactive

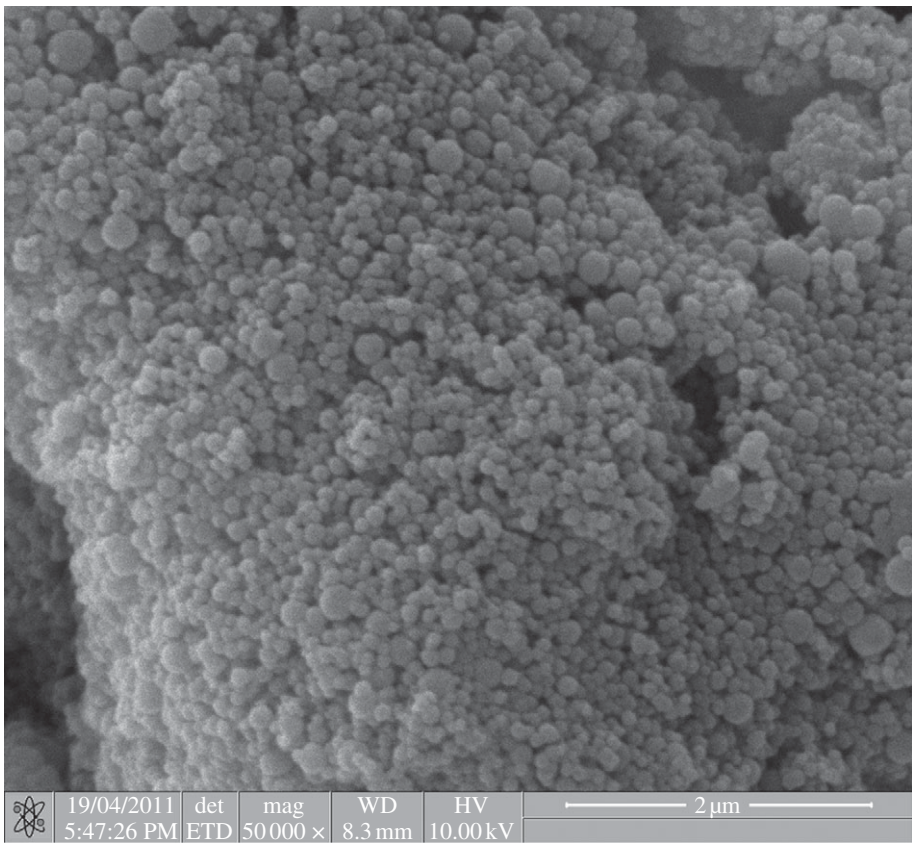

Figure 3. Bioactive MBG nanospheres prepared by hydrothermal method.

glass microspheres with a uniform diameter range of 2–5 μm and a mesoporous shell (500 nm) can be prepared by a sol–gel method using polyethylene glycol as a template [69]. Zhao *et al.* [60] prepared MBG microspheres with high P_2O_5 contents (up to 15%), and an approximate size of 4–5 μm, by using co-surfactants of P123 and CTAB. Luminescent calcium silicate MBG microspheres with a diameter of 400 nm and mesopore size of 6 nm were recently developed by Kang *et al.* [70]. Yun *et al.* [58] produced MBG nanospheres with both a large, specific surface area ($1040\ m^2\ g^{-1}$) and pore volume ($1.54\ cm^3\ g^{-1}$), and the size of MBG nanospheres can be further controlled over a diameter range of 20–200 nm by the addition of various amounts of CaO [58]. We have recently prepared novel porous MBG nanospheres (80–150 nm) by a hydrothermal method, which had excellent mineralization ability as a new intra-canal disinfectant for infected canal treatment (figure 3).

MBG can also be prepared as three-dimensional porous scaffolds by a combination of structure-directing agents and other special techniques. Currently, there are three techniques for preparing MBG scaffolds. The first MBG scaffold was prepared by the porogen method. Yun *et al.* [71] applied methylcellulose as the porogen to prepare porous MBG scaffolds with a large pore size of 100 μm. The second is the polymer template method, which is widely used. We, for the first time, prepared MBG scaffolds with a large pore size of 400 μm by using polyurethane sponge as a porous template [48]. At the same time, Li *et al.* [49] also prepared MBG scaffolds using the same method. After that, we developed a series of MBG scaffolds with varying composition for drug delivery and bone tissue engineering application (figure 4) [39,50,72,73]. The advantages of the MBG scaffolds prepared by polyurethane sponge template method are their highly interconnective pore structure and controllable pore size (porosity), while the disadvantage is the low mechanical strength of the material [51]. To better control the pore morphology, pore size and porosity, a three-dimensional plotting technique (also called direct writing or printing) has been developed to prepare porous MBG scaffolds. The significant advantage of this technique is that the architectures of the scaffolds can be concisely controlled by layer-by-layer plotting under mild conditions [74–76]. Yun *et al.* [77] and Garcia *et al.* [55] prepared hierarchical three-dimensional porous MBG scaffolds using a combination of double polymer template and rapid prototyping techniques. In their study, they mixed MBG gel with methylcellulose and then printed, sintered at 500–700°C to remove polymer templates and obtained MBG scaffolds. The main limitation of their method for preparing MBG scaffolds is the need of methylcellulose and the additional sintering procedure. Although the obtained MBG scaffolds have uniform pore structure, their mechanical strength is compromised because of the incorporation of methylcellulose, which results in some micropores. Recently, we reported a new facile method to prepare hierarchical and multi-functional MBG scaffolds with controllable pore architecture, excellent mechanical strength and mineralization ability for bone regeneration application by a modified three-dimensional printing technique using polyvinylalcohol

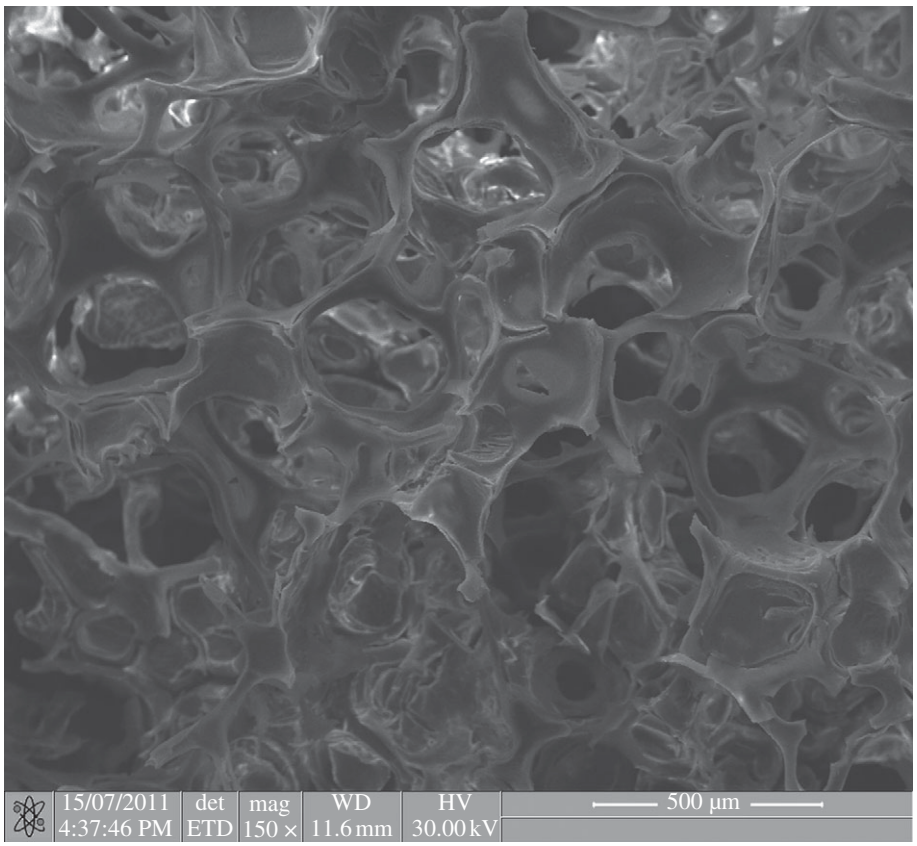

Figure 4. Porous MBG scaffolds with large pore size of around 300–500 µm prepared by the polyurethane sponge template method.

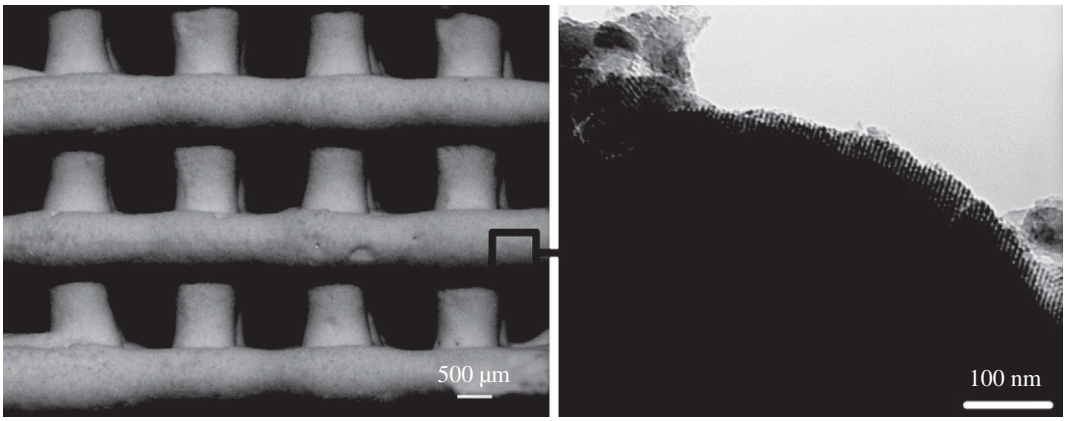

Figure 5. Three-dimensional printing MBG scaffolds with ordered large pores (several hundred micrometres) and mesopores (5 nm).

as a binder (figure 5). The obtained three-dimensional printing MBG scaffolds possess a high mechanical strength, which is about 200 times that of the MBG scaffolds prepared using the traditional polyurethane foam as template. They have highly controllable pore architecture, excellent apatite-mineralization ability and sustained drug-delivery property [78].

MBG, as bioactive phase, can be incorporated into polymers to improve their bioactivity and drug-delivery ability. The methods to prepare MBG/polymer composites mainly include direct mixing and surface coating. For this, MBG/polymer composites have been developed in the past several years. Li *et al.* [79,80] and Wei *et al.* [81] prepared MBG/poly(D,L-lactide-co-glycolide) (PLGA) and MBG/polycaprolactone composite microspheres and scaffolds with improved drug-delivery ability and *in vitro* bioactivity. MBG was used to coat on the surface of macroporous poly(L-lactic acid) (PLLA) scaffolds by Zhu *et al.* [82]. MBG coated PLLA scaffolds showed an improved bioactivity and drug-delivery property. Recently, calcium silicate-based MBG/silk composite film with excellent osteoconductivity has been prepared [83]. We have prepared a dual-drug-delivery system based on MBG/polypeptide graft copolymer nanomicelle composites [84]. MBG powders were incorporated into alginate microspheres (figure 6) and PLGA films to control drug delivery and improve the bioactivity [85,86].

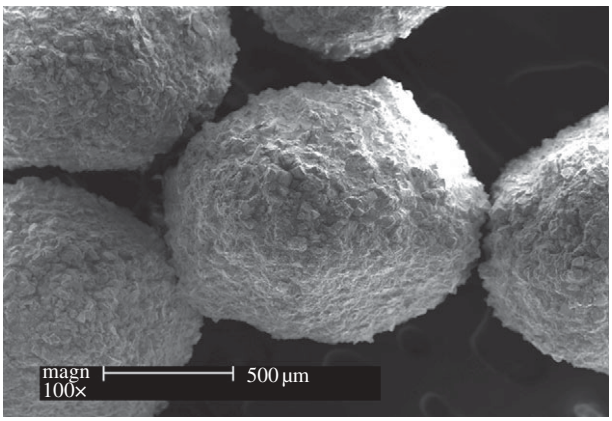

Figure 6. SEM image for MBG/alginate composite spheres for drug delivery and bone filler materials.

MBG/silk composite scaffolds were also prepared, which had improved mechanical strength and excellent *in vitro* and *in vivo* osteogenesis [51,87].

2.3. Composition–mesopore structure relationship of mesoporous bioglass materials

As pure mesoporous SiO_2 lacks adequate bioactivity, MBG has been developed with multi-components based on SiO_2–CaO or SiO_2–CaO–M_xO_y (M: P, Mg, Zn or/and Fe, etc.) to enhance the bioactivity and special functions. Generally, MBG with high contents of SiO_2 has a more ordered mesopore structure, higher specific surface area and pore volume than low-SiO_2 MBG.

The incorporation of Ca or P into mesoporous SiO_2 system significantly decreased its surface area and pore volume. Similarly, the incorporation of divalent ions (Mg, Zn, Cu or Sr), trivalent ions (Ce, Ga or B) and tetravalent ions (Zr) into SiO_2–CaO–P_2O_5 MBG system significantly decreased its mesoporous properties (surface area and pore volume; table 2). Interestingly, the composition of MBG seems to have no distinct effect on the mesopore size which is mostly in the range of 3–5 nm. The results indicated that the incorporation of additional ions into MBG system may disrupt the ordered orientation of SiO_4^{4-} during the self-assembly reaction, which may result in potential structural defects in the atomic array and further change the shape and structures of mesopores [73]. However, the MBG with varied components still possesses high surface area (in the range of 150–500 $m^2\,g^{-1}$) and pore volume (in the range of 0.2–0.6 $cm^3\,g^{-1}$; table 2).

3. DRUG/GROWTH FACTOR DELIVERY OF MESOPOROUS BIOGLASS

3.1. The effect of preparation method, composition and mesoporous bioglass forms on drug/growth factor delivery

One of the significant advantages of MBG materials is that they possess a higher specific surface area and pore volume than conventional bioactive glasses. The loading efficiency of drug and growth factors in MBG is significantly higher than that in conventional bioactive glasses [47,91]. The drug release kinetics in MBG is lower than that in conventional bioactive glasses. These characteristics make MBG useful for drug delivery. In the past several years, MBGs with different preparation methods and material forms have been used for the study of drug delivery.

The preparation method of MBG is of great importance to influence the drug delivery. Zhao *et al.* [92] used different surfactants (P123 and F127) to prepare MBG and found that P123-MBG had higher pore volume and surface area than F127-MBG. The higher pore volume and surface area of P123-MBG led to significantly higher drug (metoclopramide)-loading efficiency (47.3%), compared with that for F127-MBG (16.6%) [92]. Arcos *et al.* [28] prepared MBG by using three surfactants (CTAB, P123 and F127) and compared their drug (triclosan)-delivery ability. It was found that CTAB-induced MBG has higher loading efficiency (10.7%) than the other two MBGs (9.1% for F127 and 9.7% for P123) [28]. Therefore, it is speculated that the usage of CTAB is the better way to improve drug delivery of MBG than other surfactants.

Besides the preparation methods, the loading efficiency and release kinetics can be controlled by adjusting the composition of MBG. Zhao *et al.* [37] found that the increase in CaO content in the MBG led to the enhancement of loading efficiency and decrease of drug release rate and burst effect. The possible reason is that the drugs may be chelated with calcium on the pore wall, which makes it difficult to be released [37]. It is found that 58S MBG has slower release kinetics than 77S MBG, indicating that CaO contents in MBG play an important role in modulating the drug release [47].

The material forms are another important factor in influencing drug delivery of MBG. Table 3 summarizes the drug/growth factor category for the different forms of MBG. It can be seen that different categories of drugs and growth factors (bovine serum albumin, vascular endothelial growth factor (VEGF) and bone morphogenetic protein (BMP)) can be efficiently loaded and released in MBG particles, discs, spheres, fibres, scaffolds and composites. It is obvious that MBG forms significantly influence the loading and release of drugs and growth factors, which indicates that drug delivery in MBG is not only affected by the mesopore structures, but also the preparation methods. In addition, the release behaviour for different drugs and growth factors may be significantly different. For example, it is expected that antibiotics should keep their release behaviour constant during 5–10 days. In some cases, a burst release is required followed with sustained release. Therefore, it is of great importance to modulate the mesopore structure of MBG materials to satisfy the requirements for delivering different drugs and growth factors.

These studies suggest that MBG is an excellent drug/growth factor delivery system [47,50,98]. The potential mechanism of slow drug release kinetics of MBG is due to the existence of a large number of Si–OH groups in MBG, which plays an important role in interacting with drugs and proteins [47]. Further study has found that the drug release from MBG is mainly controlled by a Fickian diffusion mechanism

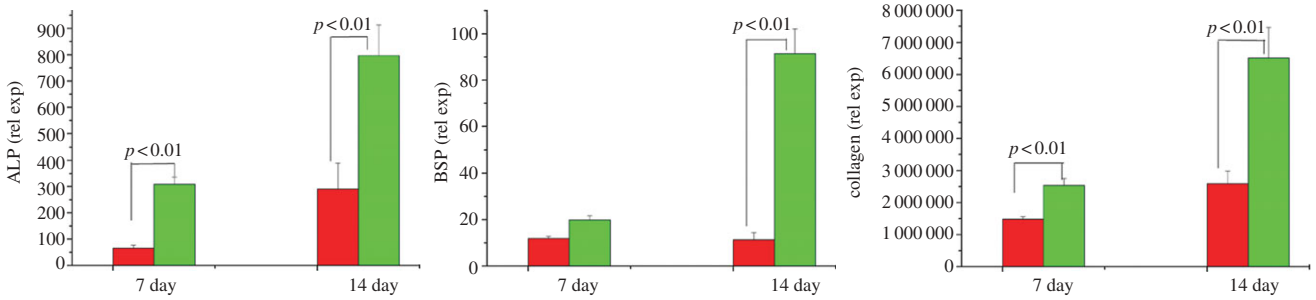

Figure 7. Dexamethasone delivery in MBG scaffolds significantly enhanced bone-relative gene expression (ALP, BSP and Col I) of human osteoblasts. Red colour bars denote MBG and green colour bars denote DEX-MBG.

Table 2. The effect of composition on the characteristics of mesopore structures.

MBG with different compositions	surface area ($m^2\,g^{-1}$)	pore volume ($cm^3\,g^{-1}$)	pore size (nm)	references
100Si	490		3.6	[52]
95Si5Ca	467		3.7	
90Si10Ca	438		3.5	
100Si	310	0.356	4.2	[55]
97.5SiP2.5 (TEP)[a]	270	0.308	4.4	
97.5SiP2.5 (H_3PO_4)[b]	152	0.235	4.8	
80Si15Ca5P	351	0.49	4.6	[41]
70Si15Ca5P	319	0.49	4.6	
60Si15Ca5P	310	0.43	4.3	
100Si	384	0.4	4.9	[48]
90Si5Ca5P	330	0.35	4.9	
80Si15Ca5P	351	0.36	4.8	
70Si25Ca5P	303	0.33	4.8	
80Si10Ca5P5Fe	260	0.26	3.5	[88]
80Si5Ca5P10Fe	334	0.3	3.6	
80Si0Ca5P15Fe	367	0.36	3.7	
80Si15Ca5P	342	0.38	3.62	[66,89]
80Si10Ca5P5Mg	274	0.35	3.31	
80Si10Ca5P5Zn	175	0.23	3.33	
80Si10Ca5P5Cu	237	0.31	3.66	
80Si10Ca5P5Sr	247	0.31	3.66	
80Si15Ca5P	515	0.58	4.7	[90]
76.5Si15Ca5P3.5Ce	397	0.38	2.9	
76.5Si15Ca5P3.5Ga	335	0.31	3.8	
80Si15Ca5P	265	0.33	5.29	[50]
75Si15Ca5P5B	234	0.24	5.28	
70Si15Ca5P10B	194	0.21	5.09	
80Si15Ca5P	317	0.37	4.1	[39]
80Si10Ca5P5Zr	287	0.32	3.7	
80Si5Ca5P10Zr	278	0.33	4.1	
80Si5P15Zr	277	0.27	3.4	

[a]97.5SiP2.5 (TEP): triethyl phosphate as the P resource.
[b]97.5SiP2.5 (H_3PO_4): H_3PO_4 as P resource.

[91]. Our recent studies further showed that the dissolution of MBG may be another important factor to influence drug release [62,72].

It is known that ordered mesoporous SiO_2 materials such as SBA-15 and MCM-41 have been widely studied as drug-delivery systems. Their characteristics such as tunable and uniform pore size, large surface area and high pore volume make it possible to adsorb drug molecules and release them from the mesostructured matrices with a sustained profile [16]. However, a recent study has shown that MBG has a higher loading efficiency and slower release rate than conventional mesoporous SiO_2 materials [37]. Since MBG materials contain different contents of CaO, CaO in the MBG leads to the enhancement of loading efficiency and a decrease in drug release rate and burst effect. One possible reason is that the drugs may be chelated with calcium on the pore wall, which makes it difficult to be released [37]; the other possible reason is that MBG has superior apatite-mineralization ability in biological solution compared with conventional mesoporous SiO_2 materials. The apatite formed on the surface of MBG materials could help

Table 3. The drug/growth factor category for MBG materials. VEGF, vascular endothelial growth factor; BMP, bone morphogenetic protein.

MBG	composition	drug/growth factor	loading efficiency (%)	burst release (%) at day 1	deliver time	references
particles	58Si36Ca6P	gentamicin	36–48	28–60	>10 days	[47,65]
	80Si15Ca5P	ibuprofen	35	25–45, 90		[88,93,94]
	80Si15Ca5P	ipriflavone	1–11			[95]
discs	100Si	tetracycline	10–18	15–30	>5 days	[37]
	90Si5Ca5P	metoclopramide	15–45	40–55		[92]
	80Si15Ca5P	phenanthrene	5.15	70		[96]
	70Si25Ca5P					
spheres	100Si	triclosan	9.1–10.7	30	>14 days	[28]
	85Si10Ca5P	ibuprofen	20	100		[70]
		bovine serum albumin	4–16	2.5–25		[62]
fibres	70Si25Ca5P	gentamicin	5.5–14.4	60–80	>4 days	[61,68]
scaffolds	80Si15Ca5P	gentamicin	11	70		[39,89,91]
	80Si15Ca5P	dexamethasone	16	20–50	>7 days	[50,51,72,73,78]
	80Si15Ca5P	VEGF	90	0.2		[97]
	100Si	BMP	—	—		[98]
composites	80Si15Ca5P	gentamicin/naproxen	1.1	30–50	>10 days	[79,82,84]
	80Si15Ca5P	dexamethasone	54	50		[85,86]

in improving drug-loading efficiency, decreasing burst release and release rate [51,62,99]. Therefore, MBG materials show improved drug-delivery ability compared with mesoporous SiO_2 materials.

3.2. The anti-bacteria and tissue-stimulation functions of the drug/growth factor-loaded mesoporous bioglass

Although there are a great number of studies for the delivery of drugs by MBG, there are few studies for the functional effect of drug/growth factor delivery from MBG. Our group has recently investigated the anti-bacterial and cell-stimulating function of drug-loaded MBG. We loaded drug ampicillin into MBG nanospheres and scaffolds and then exposed them to *Escherichia coli* (DH5α) for different time periods. It was found that the sustained release of ampicillin from MBG revealed significant anti-bacteria effect [100]. Dexamethasone (DEX) was also loaded into MBG scaffolds and it was found that the sustained release of DEX from MBG scaffolds significantly enhanced alkaline phosphatase (ALP) activity and gene expressions (Col I, Runx2, ALP and bone sialoprotein (BSP)) of osteoblasts (figure 7). These results suggest that DEX-loaded MBG scaffolds show great potential as a release system to enhance osteogenesis and may be used for bone tissue engineering application [50].

In another study, we investigated MBG scaffolds for the delivery of VEGF. It is found that MBG scaffolds have significantly higher loading efficiency and more sustained release of VEGF than NBG scaffolds, and VEGF delivery from MBG scaffolds improved the viability of endothelial cells. This study suggested that the mesopore structures in MBG scaffolds play an important role in improving the loading efficiency, decreasing the burst effect and maintaining the bioactivity of VEGF, indicating that MBG scaffolds are an excellent carrier of VEGF for potential bone tissue engineering application [97].

Recently, Dai *et al.* [98] incorporated recombinant human bone morphogenetic protein-2 (rhBMP-2) into MBG scaffolds and showed that the delivery of rhBMP-2 significantly promoted the *in vitro* osteogenic differentiation of BMSCs and induced the ectopic bone formation in the thigh muscle pouches of mice. They further found that the delivery of rhBMP-2 resulted in more bone regeneration when compared with MBG scaffolds without rhBMP-2 [98]. These studies suggest that MBG materials are a very useful carrier for drug/growth delivery with improved functions.

4. BONE REGENERATION APPLICATION OF MESOPOROUS BIOGLASS

4.1. Bioactive behaviour and mechanism of mesoporous bioglass

Another significant advantage of MBG is that it possesses superior apatite-mineralization ability in biological solution. The characteristics of MBG indicate that it may be used for bone regeneration application. In the past several years, a great number of studies have focused on the *in vitro* bioactivity of MBG with different forms, including particles and scaffolds. Yan *et al.* [41] for the first time investigated the apatite mineralization of MBG particles in SBF and found that apatite formed only after soaking for 4 h. The apatite-mineralization ability of MBG was significantly higher than that of conventional NBG. It is speculated that the highly specific surface area and pore volume of MBG play an important role in enhancing the bioactive behaviour [41]. They further optimized the composition–structure–bioactivity correlation of MBG and found that the *in vitro* bioactivity of MBG is dependent on the Si/Ca ratio in the glass network. MBG

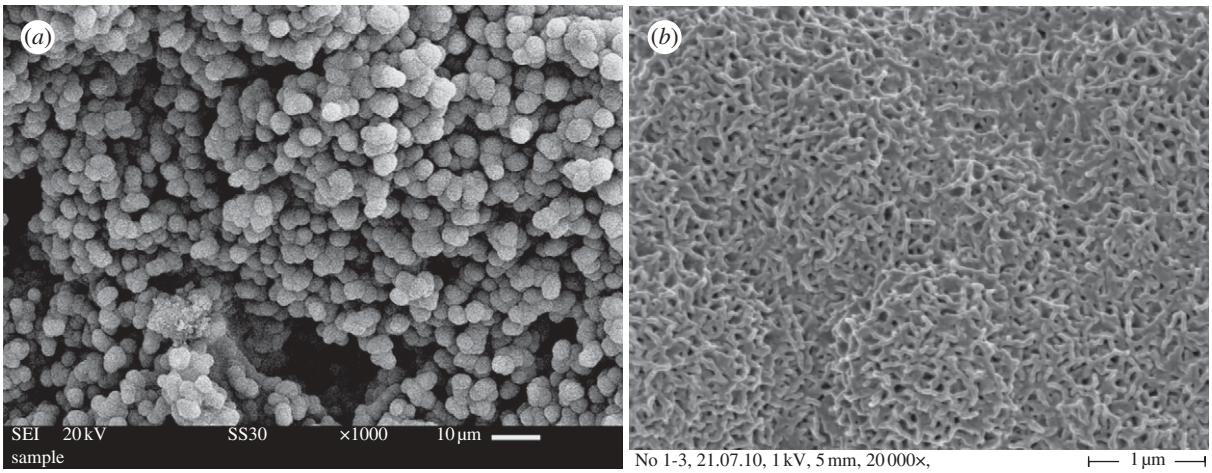

Figure 8. Nanoapatite mineralization on the surface of three-dimensional MBG scaffold: (*a*) low magnification image; (*b*) high magnification image.

(80Si15Ca5P) with relatively low calcium content exhibits the best *in vitro* bioactivity, in contrast to conventional melt NBG, where usually higher calcium percentage bioglasses (e.g. 60Si35Ca) show better bioactivity [42]. The mesopore size is also of importance to influence the apatite formation of MBG [57,101,102]. Besides the composition and mesopore size, Yan *et al.* [41] found that the mesopore morphology could affect the bioactivity of MBG. In their study, it was found that MBG-F127 with three-dimensional pore structures has improved bioactivity compared with MBG-P123 with two-dimensional hexagonal structures [41].

Garcia *et al.* studied the mechanism of apatite mineralization of MBG by using nuclear magnetic resonance spectroscopy [103]. The significant difference of the apatite formation mechanism between MBG and conventional NBG is that MBG does not require the typical 'first three stages' [103], but conventional NBG does [15]. In the first three stages, conventional NBG releases M^+ ions and forms Si–OH groups, and then Si–OH groups form networks by repolymerization. However, the surface of MBG is already inherently 'prepared' to accelerate the first three stages of the conventional NBG [103]. We investigated the bioactive behaviour of a series of three-dimensional MBG scaffolds. It is found that MBG scaffolds have improved apatite-mineralization ability (figure 8) over conventional bioglass scaffolds [50,73,78,91]. The results indicate that three-dimensional MBG scaffolds may be used for bone tissue engineering owing to their superior bioactive behaviour.

4.2. In vitro *and* in vivo *osteogenesis of mesoporous bioglass*

MBG has been regarded as a potential bioactive bone regeneration material owing to its superior bioactive behaviour. Further *in vitro* and *in vivo* osteogenesis has been studied in the past several years. We compared the attachment and viability of human osteoblasts on four-composition MBG scaffolds and found that Si80Ca15P5 MBG scaffolds had the best cell attachment [48]. MBG also supports the proliferation of human Saos-2 osteoblasts, murine L929 fibroblasts and murine SR.D10 T lymphocytes [45]. The incorporation of parts of MBG particles into PLGA enhanced the proliferation and ALP activity of human osteoblasts [85]. Our study further showed that silk modification of MBG scaffolds significantly improved the attachment (figure 9), proliferation, differentiation and osteogenic gene expression of BMSCs [51]. In addition, the incorporation of Fe, Sr, B and Zr ions into MBG scaffolds could enhance cell proliferation and osteogenic differentiation [39,50,72,73]. Interestingly, our recent study revealed that the incorporation of parts of Co^{2+} ions into MBG scaffolds significantly enhanced VEGF protein secretion, hypoxia-inducible factor-1α expression and bone-related gene expression of BMSCs. The incorporation of Co into MBG scaffolds is an efficient way to prepare hypoxia-mimicking tissue engineering scaffolds with significantly improved hypoxia function [63].

Furthermore, we incorporated MBG particles into silk scaffolds and investigated the *in vivo* osteogenesis. The study showed that MBG/silk scaffolds induced a higher rate of type I collagen synthesis and new bone formation after implantation in rat calvarial defects, compared with conventional NBG/silk scaffolds. The results confirm that MBG—a new class of bioactive inorganic materials—has significant capacity to improve the *in vivo* bioactivity of polymer-based scaffolds [87]. Recently, we implanted three-dimensional printed MBG scaffolds into the defects of rat femur. After four weeks of implantation, MBG scaffolds induced a great amount of new bone ingrowths in the defects (figure 10). The results further indicate that MBG has excellent *in vivo* osteogenesis for potential bone repair application. Up to now, there is no report of the effect of different preparation methods of MBG scaffolds (porogen methods, polyurethane sponge template method and three-dimensional printed method) on their *in vitro* and *in vivo* osteogenesis. However, considering the physico-chemical properties (e.g. pore structure and mechanical strength) of the obtained MBG scaffolds by these methods, three-dimensional printing MBG scaffolds possess a high mechanical strength that is about 200 times of that of the MBG scaffolds prepared using traditional polyurethane foam as template. They

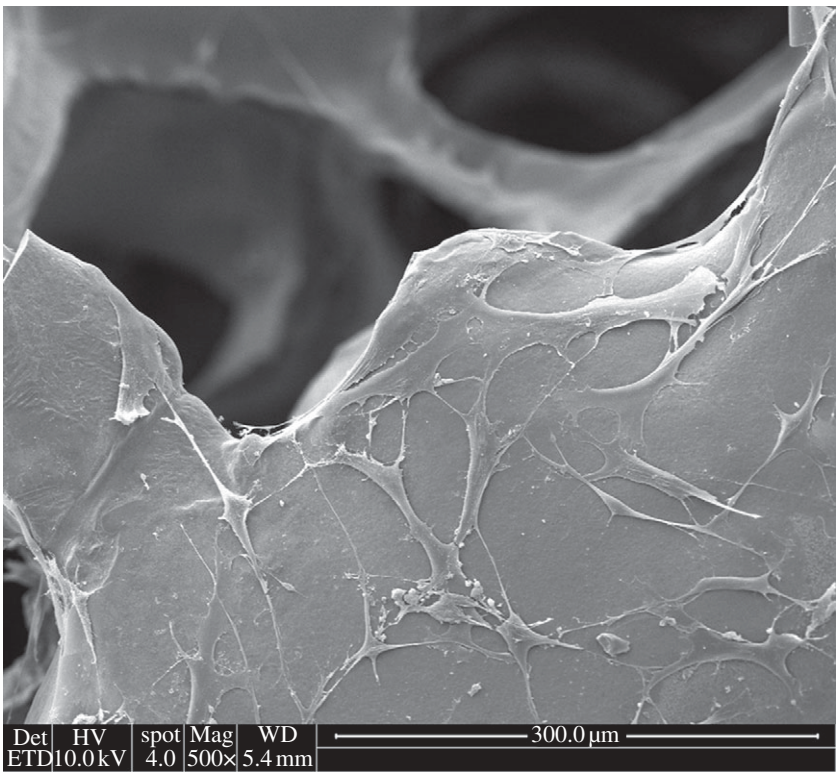

Figure 9. BMSC attachment on silk-modified MBG scaffolds.

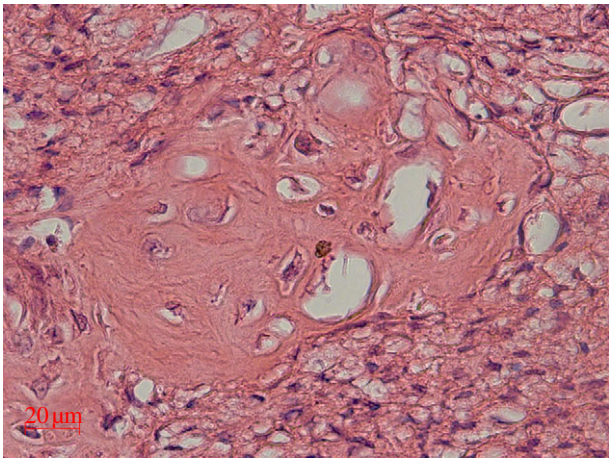

Figure 10. The *in vivo* bone formation was evaluated by haematoxylin and eosin staining of MBG scaffolds in the femur defects of rats.

have highly controllable pore architecture, excellent apatite-mineralization ability and sustained drug-delivery property [78]. Furthermore, the three-dimensional printing technique could also be widely used for preparing MBG-containing composite scaffolds. Therefore, three-dimensional-printed MBG scaffolds may be one of the options for bone tissue engineering application.

5. CONCLUSION AND PERSPECTIVE

In this article, we reviewed the recent research advances of a new class of bioactive glasses, named as MBGs, in the past several years. We summarized the preparation methods, the effect of mesopore templates and composition on the mesopore–structure characteristics, and different forms of MBG materials, including particles, fibres, spheres, scaffolds and composites. In addition, MBG, as a potential drug/growth factor carrier, was reviewed, which includes the composition–structure–drug-delivery relationship and the functional effect on the anti-bacteria and tissue-stimulation properties. Furthermore, the bioactivity, *in vitro* and *in vivo* osteogenesis of MBG are highlighted. Generally, MBGs offer a suite of features that are important for efficient drug delivery and bone regeneration. The typical features include the following. (i) They possess well-ordered mesoporous channel structure and controllable nanopore size, which endows them with a highly specific surface area and pore volume. The improved physical properties play an important role in enhancing their biological behaviour. (ii) They have excellent *in vitro* and *in vivo* bioactivity. Particularly, they have shown the stimulatory effect to enhance *in vivo* bone formation, compared with NBG. (iii) They are excellent carriers for the delivery of drugs and growth factors to further improve anti-bacteria ability and stimulate the growth and differentiation of tissue cells as well as bone tissue formation. The typical advantages and limitations of MBG are summarized in table 4.

To our knowledge, it is difficult to load drugs in NBGs or other bioceramics with a loading efficiency higher than 15 per cent; however, mesoporous structure could significantly improve the loading efficiency of the drugs in MBGs. Our studies have shown that the drug-loading efficiency for MBG particles could reach 50 per cent. Even MBG scaffolds could load drugs with 20 per cent loading efficiency. Therefore, for MBGs, they could be regarded as drug-delivery materials with high loading efficiency. In addition, the preparation methods of MBG play an important role in influencing the mesopore

Table 4. The main advantages and limitations of MBG by comparing with microsize bioactive glasses and nanosize bioactive glasses.

applications		MBG	microsize bioactive glasses	nanosize bioactive glasses
microstructure	advantages	mesoporous channel (2–20 nm), high surface area and pore volume		nanosize particles, high surface area
	limitations	limited pore size (<20 nm)	lack nanostructures, low surface area and pore volume	low pore size
drug delivery	advantages	high loading efficiency, sustained release		a certain loading efficiency
	limitations		low loading efficiency (<15), burst release	uncontrollable release
bone tissue engineering	advantages	superior bioactivity	good bioactivity	excellent bioactivity
	limitations	mechanical strength	mechanical strength	hard to form scaffolds

structure, drug delivery and bone tissue engineering application. Generally, CTAB-induced MBG has improved drug-delivery properties over P123- and F127-induced MBG. For bone tissue engineering application, the three-dimensional-printed method has more advantages to control large pore structure and mechanical strength of MBG scaffolds than other methods.

It is of great significance to study MBG materials for drug delivery and bone tissue engineering application. The study will provide fundamental knowledge of how to combine nanotechnology and material science with biomedical engineering, which is a typical interdisciplinary research. MBG materials possess both drug delivery and superior bioactivity, which show great potential for clinical application. It is believed that the combination of efficient drug delivery and inherent osteogenesis of MBG will provide more options to treat bone-related defects clinically.

The important issues such as the mechanism of *in vivo* bone formation, degradation and metabolism have to be investigated before further clinical trials. With further understanding of the biological activity and corresponding mechanism of MBG *in vivo*, it is expected that MBG may be a promising biomaterial for clinical application in the coming ten years. For this aim, it is suggested that the potential directions for the study of MBG should include the following. (i) Large animal models should be used to further investigate the *in vivo* osteogenesis and degradation of MBG. (ii) Our studies have shown that some drugs can be efficiently delivered using an MBG system and are capable of significantly enhancing its *in vitro* bioactivity. These findings provide the new paradigm that osteoinductive drugs may be preloaded into an MBG scaffold system to stimulate *in vitro* and *in vivo* osteogenesis for the purposes of bone tissue engineering. However, the effect of drug delivery on the *in vivo* osteogenesis is unclear, and further studies need to be conducted in the future. (iii) MBG nanospheres may be used as an injectable drug carrier for treating bone and dental diseases, as they combine bioactivity and drug-delivery property.

The authors thank One Hundred Talent Project, SIC-CAS and the Natural Science Foundation of China (grant no. 30730034) for the support of this research.

REFERENCES

1 Misra, S. K. *et al.* 2010 Effect of nanoparticulate bioactive glass particles on bioactivity and cytocompatibility of poly(3-hydroxybutyrate) composites. *J. R. Soc. Interface* **7**, 453–465. (doi:10.1098/rsif.2009.0255)
2 Hench, L. L. & Thompson, I. 2010 Twenty-first century challenges for biomaterials. *J. R. Soc. Interface* **7**(Suppl 4), S379–S391. (doi:10.1098/rsif.2010.0151.focus)
3 Chen, Q. Z., Thompson, I. D. & Boccaccini, A. R. 2006 45S5 Bioglass-derived glass–ceramic scaffolds for bone tissue engineering. *Biomaterials* **27**, 2414–2425. (doi:10.1016/j.biomaterials.2005.11.025)
4 Jones, J. R., Tsigkou, O., Coates, E. E., Stevens, M. M., Polak, J. M. & Hench, L. L. 2007 Extracellular matrix formation and mineralization on a phosphate-free porous bioactive glass scaffold using primary human osteoblast (HOB) cells. *Biomaterials* **28**, 1653–1663. (doi:10.1016/j.biomaterials.2006.11.022)
5 Jones, J. R., Ehrenfried, L. M. & Hench, L. L. 2006 Optimising bioactive glass scaffolds for bone tissue engineering. *Biomaterials* **27**, 964–973. (doi:10.1016/j.biomaterials.2005.07.017)
6 Wu, Z. Y., Hill, R. G., Yue, S., Nightingale, D., Lee, P. D. & Jones, J. R. 2011 Melt-derived bioactive glass scaffolds produced by a gel-cast foaming technique. *Acta Biomater.* **7**, 1807–1816. (doi:10.1016/j.actbio.2010.11.041)
7 Hench, L. L. 1991 Bioceramics: from concept to clinic. *J. Am. Ceram. Soc.* **74**, 1487–1510. (doi:10.1111/j.1151-2916.1991.tb07132.x)
8 Hench, L. L. 1998 Biomaterials: a forecast for the future. *Biomaterials* **19**, 1419–1423. (doi:10.1016/S0142-9612(98)00133-1)
9 Gough, J. E., Jones, J. R. & Hench, L. L. 2004 Nodule formation and mineralisation of human primary osteoblasts cultured on a porous bioactive glass scaffold. *Biomaterials* **25**, 2039–2046. (doi:10.1016/j.biomaterials.2003.07.001)
10 Gough, J. E., Notingher, I. & Hench, L. L. 2004 Osteoblast attachment and mineralized nodule formation on rough and smooth 45S5 bioactive glass monoliths. *J. Biomed. Mater. Res. A* **68**, 640–650. (doi:10.1002/jbm.a.20075)
11 Valerio, P., Pereira, M. M., Goes, A. M. & Leite, M. F. 2004 The effect of ionic products from bioactive glass dissolution on osteoblast proliferation and collagen production. *Biomaterials* **25**, 2941–2948. (doi:10.1016/j.biomaterials.2003.09.086)
12 Xynos, I. D., Edgar, A. J., Buttery, L. D., Hench, L. L. & Polak, J. M. 2000 Ionic products of bioactive glass

dissolution increase proliferation of human osteoblasts and induce insulin-like growth factor II mRNA expression and protein synthesis. *Biochem. Biophys. Res. Commun.* **276**, 461–465. (doi:10.1006/bbrc.2000.3503)
13 Hoppe, A., Guldal, N. S. & Boccaccini, A. R. 2011 A review of the biological response to ionic dissolution products from bioactive glasses and glass-ceramics. *Biomaterials* **32**, 2757–2774. (doi:10.1016/j.biomaterials.2011.01.004)
14 Wu, C., Chang, J. & Xiao, Y. 2011 Mesoporous bioactive glasses as drug delivery and bone tissue engineering platforms. *Ther. Deliv.* **2**, 1189–1198. (doi:10.4155/tde.11.84)
15 Hench, L. L. & Polak, J. M. 2002 Third-generation biomedical materials. *Science* **295**, 1014–1017. (doi:10.1126/science.1067404)
16 Arcos, D. & Vallet-Regi, M. 2010 Sol–gel silica-based biomaterials and bone tissue regeneration. *Acta Biomater.* **6**, 2874–2888. (doi:10.1016/j.actbio.2010.02.012)
17 Abou Neel, E. A., Chrzanowski, W. & Knowles, J. C. 2008 Effect of increasing titanium dioxide content on bulk and surface properties of phosphate-based glasses. *Acta Biomater.* **4**, 523–534. (doi:10.1016/j.actbio.2007.11.007)
18 Abou Neel, E. A., Chrzanowski, W., Valappil, S. P., O'Dell, L. A., Pickup, D. M., Smith, M. E., Newport, R. J. & Knowles, J. C. 2009 Doping of a high calcium oxide metaphosphate glass with titanium dioxide. *J. Non-Cryst. Solids* **355**, 991–1000. (doi:10.1016/j.jnoncrysol.2009.04.016)
19 Abou Neel, E. A., Ahmed, I., Blaker, J. J., Bismarck, A., Boccaccini, A. R., Lewis, M. P., Nazhat, S. N. & Knowles, J. C. 2005 Effect of iron on the surface, degradation and ion release properties of phosphate-based glass fibres. *Acta Biomater.* **1**, 553–563. (doi:10.1016/j.actbio.2005.05.001)
20 Pietak, A. M., Reid, J. W., Stott, M. J. & Sayer, M. 2007 Silicon substitution in the calcium phosphate bioceramics. *Biomaterials* **28**, 4023–4032. (doi:10.1016/j.biomaterials.2007.05.003)
21 Bohner, M. 2009 Silicon-substituted calcium phosphates: a critical view. *Biomaterials* **30**, 6403–6406. (doi:10.1016/j.biomaterials.2009.08.007)
22 Mastrogiacomo, M., Muraglia, A., Komlev, V., Peyrin, F., Rustichelli, F., Crovace, A. & Cancedda, R. 2005 Tissue engineering of bone: search for a better scaffold. *Orthod. Craniofac. Res.* **8**, 277–284. (doi:10.1111/j.1601-6343.2005.00350.x)
23 Laurencin, D. *et al.* 2011 Magnesium incorporation into hydroxyapatite. *Biomaterials* **32**, 1826–1837. (doi:10.1016/j.biomaterials.2010.11.017)
24 Li, R., Clark, A. E. & Hench, L. L. 1991 An investigation of bioactive glass powders by sol–gel processing. *J. Appl. Biomater.* **2**, 231–239. (doi:10.1002/jab.770020403)
25 Cerruti, M. & Sahai, N. 2006 Silicate biomaterials for orthopaedic and dental implants. *Rev. Mineral. Geochem.* **64**, 283–313. (doi:10.2138/rmg.2006.64.9)
26 Zhong, J. & Greenspan, D. C. 2000 Processing and properties of sol–gel bioactive glasses. *J. Biomed. Mater. Res.* **53**, 694–701. (doi:10.1002/1097-4636(2000)53:6<694::AID-JBM12>3.0.CO;2-6)
27 Hamadouche, M., Meunier, A., Greenspan, D. C., Blanchat, C., Zhong, J. P., La Torre, G. P. & Sedel, L. 2001 Long-term *in vivo* bioactivity and degradability of bulk sol–gel bioactive glasses. *J. Biomed. Mater. Res.* **54**, 560–566. (doi:10.1002/1097-4636(20010315)54:4<560::AID-JBM130>3.0.CO;2-J)
28 Arcos, D., Lopez-Noriega, A., Ruiz-Hernandez, E., Terasaki, O. & Vallet-Regi, M. 2009 Ordered mesoporous microspheres for bone grafting and drug delivery. *Chem. Mater.* **21**, 1000–1009. (doi:10.1021/cm801649z)
29 Zhao, D., Feng, J., Huo, Q., Melosh, N., Fredrickson, G. H., Chmelka, B. F. & Stucky, G. D. 1998 Triblock copolymer syntheses of mesoporous silica with periodic 50 to 300 angstrom pores. *Science* **279**, 548–552. (doi:10.1126/science.279.5350.548)
30 Lopez-Noriega, A., Arcos, D., Izquierdo-Barb, I., Sakamoto, Y., Terasaki, O. & Vallet-Regi, M. 2006 Ordered mesoporous bioactive glasses for bone tissue regeneration. *Chem. Mater.* **18**, 3137–3144. (doi:10.1021/cm060488o)
31 Vallet-Regi, M. 2006 Revisiting ceramics for medical applications. *Dalton Trans.* 5211–5220. (doi:10.1039/b610219k)
32 Vallet-Regi, M. A., Ruiz-Gonzalez, L., Izquierdo-Barba, I. & Gonzalez-Calbet, J. M. 2006 Revisiting silica based ordered mesoporous materials: medical applications. *J. Mater. Chem.* **16**, 26–31. (doi:10.1039/b509744d)
33 Manzanoab, M. & Vallet-Regi, M. 2010 New developments in ordered mesoporous materials for drug delivery. *J. Mater. Chem.* **20**, 5593–5604. (doi:10.1039/b922651f)
34 Vallet-Regi, M., Balas, F. & Arcos, D. 2007 Mesoporous materials for drug delivery. *Angew. Chem. Int. Ed. Engl.* **46**, 7548–7558. (doi:10.1002/anie.200604488)
35 Horcajada, P., Ramila, A., Boulahya, K., Gonzalez-Calbet, J. & Vallet-Regi, M. 2004 Bioactivity in ordered mesoporous materials. *Solid State Sci.* **6**, 1295–1300. (doi:10.1016/j.solidstatesciences.2004.07.026)
36 Izquierdo-Barba, I., Ruiz-Gonzalez, L., Doadrio, J. C., Gonzalez-Calbet, J. M. & Vallet-Regi, M. 2005 Tissue regeneration: a new property of mesoporous materials. *Solid State Sci.* **7**, 983–989. (doi:10.1016/j.solidstatesciences.2005.04.003)
37 Zhao, L. Z., Yan, X. X., Zhou, X. F., Zhou, L., Wang, H. N., Tang, H. W. & Yu, C. Z. 2008 Mesoporous bioactive glasses for controlled drug release. *Microporous Mesoporous Mater.* **109**, 210–215. (doi:10.1016/j.micromeso.2007.04.041)
38 Mourino, V. & Boccaccini, A. R. 2009 Bone tissue engineering therapeutics: controlled drug delivery in three-dimensional scaffolds. *J. R. Soc. Interface* **7**, 209–227. (doi:10.1098/rsif.2009.0379)
39 Zhu, Y., Zhang, Y., Wu, C., Fang, Y., Wang, J. & Wang, S. 2011 The effect of zirconium incorporation on the physiochemical and biological properties of mesoporous bioactive glasses scaffolds. *Microporous Mesoporous Mater.* **143**, 311–319. (doi:10.1016/j.micromeso.2011.03.007)
40 Vallet-Regi, M. 2006 Ordered mesoporous materials in the context of drug delivery systems and bone tissue engineering. *Chem. Eur. J.* **12**, 5934–5943. (doi:10.1002/chem.200600226)
41 Yan, X., Yu, C., Zhou, X., Tang, J. & Zhao, D. 2004 Highly ordered mesoporous bioactive glasses with superior *in vitro* bone-forming bioactivities. *Angew. Chem. Int. Ed. Engl.* **43**, 5980–5984. (doi:10.1002/anie.200460598)
42 Yan, X., Huang, X., Yu, C., Deng, H., Wang, Y., Zhang, Z., Qiao, S., Lu, G. & Zhao, D. 2006 The *in-vitro* bioactivity of mesoporous bioactive glasses. *Biomaterials* **27**, 3396–3403. (doi:10.1016/j.biomaterials.2006.01.043)
43 Leonova, E., Izquierdo-Barba, I., Arcos, D., Lopez-Noriega, A., Hedin, N., Vallet-Regi, M. & Eden, M. 2008 Multinuclear solid-state NMR studies of ordered mesoporous bioactive glasses. *J. Phys. Chem. C* **112**, 5552–5562. (doi:10.1021/jp7107973)
44 Garcia, A., Cicuendez, M., Izquierdo-Barba, I., Arcos, D. & Vallet-Regi, M. 2009 Essential role of calcium phosphate heterogeneities in 2D-hexagonal and 3D-cubic SiO_2–CaO–P_2O_5 mesoporous bioactive glasses. *Chem. Mater.* **21**, 5474–5484. (doi:10.1021/cm9022776)
45 Alcaide, M., Portoles, P., Lopez-Noriega, A., Arcos, D., Vallet-Regi, M. & Portoles, M. T. 2010 Interaction of an

ordered mesoporous bioactive glass with osteoblasts, fibroblasts and lymphocytes, demonstrating its biocompatibility as a potential bone graft material. *Acta Biomater.* **6**, 892–899. (doi:10.1016/j.actbio.2009.09.008)

46 Brinker, C. J., Lu, Y. F., Sellinger, A. & Fan, H. Y. 1999 Evaporation-induced self-assembly: nanostructures made easy. *Adv. Mater.* **11**, 579–585. (doi:10.1002/(SICI)1521-4095(199905)11:7<579::AID-ADMA579>3.0.CO;2-R)

47 Xia, W. & Chang, J. 2006 Well-ordered mesoporous bioactive glasses (MBG): a promising bioactive drug delivery system. *J. Control. Release* **110**, 522–530. (doi:10.1016/j.jconrel.2005.11.002)

48 Zhu, Y., Wu, C., Ramaswamy, Y., Kockrick, E., Simon, P., Kaskel, S. & Zreiqat, H. 2008 Preparation, characterization and *in vitro* bioactivity of mesoporous bioactive glasses (MBGs) scaffolds for bone tissue engineering. *Microporous Mesoporous Mater.* **112**, 494–503. (doi:10.1016/j.micromeso.2007.10.029)

49 Li, X., Wang, X. P., Chen, H. R., Jiang, P., Dong, X. P. & Shi, J. L. 2007 Hierarchically porous bioactive glass scaffolds synthesized with a PUF and P123 cotemplated approach. *Chem. Mater.* **19**, 4322–4326. (doi:10.1021/cm0708564)

50 Wu, C., Miron, R., Sculeaan, A., Kaskel, S., Doert, T., Schulze, R. & Zhang, Y. 2011 Proliferation, differentiation and gene expression of osteoblasts in boron-containing associated with dexamethasone deliver from mesoporous bioactive glass scaffolds. *Biomaterials* **32**, 7068–7078. (doi:10.1016/j.biomaterials.2011.06.009)

51 Wu, C., Zhang, Y., Zhu, Y., Friis, T. & Xiao, Y. 2010 Structure–property relationships of silk-modified mesoporous bioglass scaffolds. *Biomaterials* **31**, 3429–3438. (doi:10.1016/j.biomaterials.2010.01.061)

52 Wu, X., Wei, J., Lu, X., Lv, Y., Chen, F., Zhang, Y. & Liu, C. 2010 Chemical characteristics and hemostatic performances of ordered mesoporous calcium-doped silica xerogels. *Biomed. Mater.* **5**, 035006. (doi:10.1088/1748-6041/5/3/035006)

53 Wang, J. Q., Yan, P. H., Liu, S., Ou, J. F., Lei, Z. Q. & Yang, S. R. 2010 'Green' synthesis of highly ordered mesoporous bioactive glass using acetic anhydride as the catalyst. *J. Non-Cryst. Solids* **356**, 1514–1518. (doi:10.1016/j.jnoncrysol.2010.05.058)

54 Yun, H. S., Kim, S. E. & Hyun, Y. T. 2008 Preparation of 3D cubic ordered mesoporous bioactive glasses. *Solid State Sci.* **10**, 1083–1092. (doi:10.1016/j.solidstatesciences.2007.11.037)

55 Garcia, A., Izquierdo-Barba, I., Colilla, M., de Laorden, C. L. & Vallet-Regi, M. 2011 Preparation of 3-D scaffolds in the SiO_2–P_2O_5 system with tailored hierarchical meso-macroporosity. *Acta Biomater.* **7**, 1265–1273. (doi:10.1016/j.actbio.2010.10.006)

56 Yun, H. S., Kim, S. E. & Hyun, Y. T. 2009 Preparation of bioactive glass ceramic beads with hierarchical pore structure using polymer self-assembly technique. *Mater. Chem. Phys.* **115**, 670–676. (doi:10.1016/j.matchemphys.2009.02.001)

57 Yu, C. Z., Yan, X. X., Wei, G. F., Zhao, L. Z., Yi, J., Deng, H. X., Wang, L. Z. & Lu, G. Q. 2010 Synthesis and *in vitro* bioactivity of ordered mesostructured bioactive glasses with adjustable pore sizes. *Microporous Mesoporous Mater.* **132**, 282–289. (doi:10.1016/j.micromeso.2010.03.009)

58 Yun, H. S., Kim, S. H., Lee, S. & Song, I. H. 2010 Synthesis of high surface area mesoporous bioactive glass nanospheres. *Mater. Lett.* **64**, 1850–1853. (doi:10.1016/j.matlet.2010.04.053)

59 Wu, C., Fan, W., Chang, J. & Xiao, Y. Submitted. Mesoporous bioglass nanospheres for anti-cancer drug delivery.

60 Zhao, S., Li, Y. B. & Li, D. X. 2010 Synthesis and *in vitro* bioactivity of CaO–SiO_2–P_2O_5 mesoporous microspheres. *Microporous Mesoporous Mater.* **135**, 67–73. (doi:10.1016/j.micromeso.2010.06.012)

61 Hong, Y., Chen, X., Jing, X., Fan, H., Guo, B., Gu, Z. & Zhang, X. 2010 Preparation, bioactivity, and drug release of hierarchical nanoporous bioactive glass ultrathin fibers. *Adv. Mater.* **22**, 754–758. (doi:10.1002/adma.200901656)

62 Wu, C., Zhang, Y., Ke, X., Xie, Y., Zhu, H., Crawford, R. & Xiao, Y. 2010 Bioactive mesopore-glass microspheres with controllable protein-delivery properties by biomimetic surface modification. *J. Biomed. Mater. Res. A* **95**, 476–485. (doi:10.1002/jbm.a.32873)

63 Wu, C., Zhou, Y., Fan, W., Han, P., Chang, J., Yuen, J., Zhang, M. & Xiao, Y. 2012 Hypoxia-mimicking mesoporous bioactive glass scaffolds with controllable cobalt ion release for bone tissue engineering. *Biomaterials* **33**, 2076–2085. (doi:10.1016/j.biomaterials.2011.11.042)

64 Lei, B., Chen, X. F., Wang, Y. J., Zhao, N., Du, C. & Zhang, L. M. 2009 Acetic acid derived mesoporous bioactive glasses with an enhanced *in vitro* bioactivity. *J. Non-Cryst. Solids* **355**, 2583–2587. (doi:10.1016/j.jnoncrysol.2009.09.014)

65 Xia, W. & Chang, J. 2008 Preparation, *in vitro* bioactivity and drug release property of well-ordered mesoporous 58S bioactive glass. *J. Non-Cryst. Solids* **15**, 1338–1341. (doi:10.1016/j.jnoncrysol.2006.10.084)

66 Li, X., Wang, X. P., He, D. N. & Shi, J. L. 2008 Synthesis and characterization of mesoporous CaO-MO-SiO_2-P_2O_5 (M=Mg, Zn, Cu) bioactive glasses/composites. *J. Mater. Chem.* **18**, 4103–4109. (doi:10.1039/b805114c)

67 Feng, X. & Chang, J. 2011 Synthesis of a well-ordered mesoporous 58S bioactive glass by a simple method. *Int. J. Appl. Ceram. Technol.* **8**, 547–552. (doi:10.1111/j.1744-7402.2010.02596.x)

68 Hong, Y. L., Chen, X. S., Jing, X. B., Fan, H. S., Gu, Z. W. & Zhang, X. D. 2010 Fabrication and drug delivery of ultrathin mesoporous bioactive glass hollow fibers. *Adv. Funct. Mater.* **20**, 1503–1510. (doi:10.1002/adfm.200901627)

69 Lei, B., Chen, X. F., Wang, Y. J. & Zhao, N. 2009 Synthesis and *in vitro* bioactivity of novel mesoporous hollow bioactive glass microspheres. *Mater. Lett.* **63**, 1719–1721. (doi:10.1016/j.matlet.2009.04.041)

70 Kang, X., Huang, S., Yang, P., Ma, P., Yang, D. & Lin, J. 2011 Preparation of luminescent and mesoporous Eu^{3+}/Tb^{3+} doped calcium silicate microspheres as drug carriers via a template route. *Dalton Trans.* **40**, 1873–1879. (doi:10.1039/c0dt01390k)

71 Yun, H., Kim, S. E., Hyun, Y. T., Heo, S. & Shin, J. 2008 Hierarchically mesoporous–macroporous bioactive glasses scaffolds for bone tissue regeneration. *J. Biomed. Mater. Res. B* **87B**, 374–380. (doi:10.1002/jbm.b.31114)

72 Wu, C., Fan, W., Gelinsky, M., Xiao, Y., Simon, P., Schulze, R., Doert, T., Luo, Y. & Cuniberti, G. 2011 Bioactive SrO–SiO_2 glass with well-ordered mesopores: characterization, physiochemistry and biological properties. *Acta Biomater.* **7**, 1797–1806. (doi:10.1016/j.actbio.2010.12.018)

73 Wu, C., Fan, W., Zhu, Y., Gelinsky, M., Chang, J., Cuniberti, G., Albrecht, V., Friis, T. & Xiao, Y. 2011 Multifunctional magnetic mesoporous bioactive glass scaffolds with a hierarchical pore structure. *Acta Biomater.* **7**, 3563–3572. (doi:10.1016/j.actbio.2011.06.028)

74 Franco, J., Hunger, P., Launey, M. E., Tomsia, A. P. & Saiz, E. 2010 Direct write assembly of calcium phosphate

scaffolds using a water-based hydrogel. *Acta Biomater.* **6**, 218–228. (doi:10.1016/j.actbio.2009.06.031)

75 Miranda, P., Pajares, A., Saiz, E., Tomsia, A. P. & Guiberteau, F. 2008 Mechanical properties of calcium phosphate scaffolds fabricated by robocasting. *J. Biomed. Mater. Res. A* **85A**, 218–227. (doi:10.1002/jbm.a.31587)

76 Miranda, P., Saiz, E., Gryn, K. & Tomsia, A. P. 2006 Sintering and robocasting of β-tricalcium phosphate scaffolds for orthopaedic applications. *Acta Biomater.* **2**, 457–466. (doi:10.1016/j.actbio.2006.02.004)

77 Yun, H. S., Kim, S. E. & Hyeon, Y. T. 2007 Design and preparation of bioactive glasses with hierarchical pore networks. *Chem. Commun.* 2139–2141. (doi:10.1039/b702103h)

78 Wu, C., Luo, Y., Cuniberti, G., Xiao, Y. & Gelinsky, M. 2011 Three-dimensional printing of hierarchical and tough mesoporous bioactive glass scaffolds with a controllable pore architecture, excellent mechanical strength and mineralization ability. *Acta Biomater.* **7**, 2644–2650. (doi:10.1016/j.actbio.2011.03.009)

79 Li, X., Wang, X., Zhang, L., Chen, H. & Shi, J. 2009 MBG/PLGA composite microspheres with prolonged drug release. *J. Biomed. Mater. Res. B* **89B**, 148–154. (doi:10.1002/jbm.b.31197)

80 Li, X., Shi, J., Dong, X., Zhang, L. & Zeng, H. 2008 A mesoporous bioactive glass/polycaprolactone composite scaffold and its bioactivity behavior. *J. Biomed. Mater. Res. A* **84A**, 84–91. (doi:10.1002/jbm.a.31371)

81 Wei, J., Chen, F., Shin, J. W., Hong, H., Dai, C., Su, J. & Liu, C. 2009 Preparation and characterization of bioactive mesoporous wollastonite: polycaprolactone composite scaffold. *Biomaterials* **30**, 1080–1088. (doi:10.1016/j.biomaterials.2008.10.046)

82 Zhu, M., Zhang, L. X., He, Q. J., Zhao, J. J., Guo, L. M. & Shi, J. L. 2011 Mesoporous bioactive glass-coated poly(L-lactic acid) scaffolds: a sustained antibiotic drug release system for bone repairing. *J. Mater. Chem.* **21**, 1064–1072. (doi:10.1039/c0jm02179b)

83 Zhu, H., Wu, B., Feng, X. & Chen, J. 2011 Preparation and characterization of bioactive mesoporous calcium silicate–silk fibroin composite films. *J. Biomed. Mater. Res. B* **98B**, 330–341. (doi:10.1002/jbm.b.31856)

84 Xia, W., Chang, J., Lin, J. & Zhu, J. 2008 The pH-controlled dual-drug release from mesoporous bioactive glass/polypeptide graft copolymer nanomicelle composites. *Eur. J. Pharm. Biopharm.* **69**, 546–552. (doi:10.1016/j.ejpb.2007.11.018)

85 Wu, C., Ramaswamy, Y., Zhu, Y., Zheng, R., Appleyard, R., Howard, A. & Zreiqat, H. 2009 The effect of mesoporous bioactive glass on the physiochemical, biological and drug-release properties of poly(DL-lactide-co-glycolide) films. *Biomaterials* **30**, 2199–2208. (doi:10.1016/j.biomaterials.2009.01.029)

86 Wu, C., Zhu, Y., Chang, J., Zhang, Y. & Xiao, Y. 2010 Bioactive inorganic-materials/alginate composite microspheres with controllable drug-delivery ability. *J. Biomed. Mater. Res. B* **94B**, 32–43. (doi:10.1002/jbm.b.31621)

87 Wu, C., Zhang, Y., Zhou, Y., Fan, W. & Xiao, Y. 2011 A comparative study of mesoporous-glass/silk and non-mesoporous-glass/silk scaffolds: physiochemistry and *in vivo* osteogenesis. *Acta Biomater.* **7**, 2229–2236. (doi:10.1016/j.actbio.2010.12.019)

88 Li, X., Wang, X. P., Hua, Z. L. & Shi, J. L. 2008 One-pot synthesis of magnetic and mesoporous bioactive glass composites and their sustained drug release property. *Acta Mater.* **56**, 3260–3265. (doi:10.1016/j.actamat.2008.03.013)

89 Zhu, Y., Li, X., Yang, J., Wang, S., Gao, H. & Hanagata, N. 2011 Composition–structure–property relationship of the $CaO–M_xO_y–SiO_2–P_2O_5$ (M=Zr, Mg, Sr) mesoporous bioactive glass (MBG) scaffolds. *J. Mater. Chem.* **21**, 9208–9218. (doi:10.1039/c1jm10838g)

90 Salinas, A. J., Shruti, S., Malavasi, G., Menabue, L. & Vallet-Regi, M. 2011 Substitutions of cerium, gallium and zinc in ordered mesoporous bioactive glasses. *Acta Biomater.* **7**, 3452–3458. (doi:10.1016/j.actbio.2011.05.033)

91 Zhu, Y. F. & Kaskel, S. 2009 Comparison of the *in vitro* bioactivity and drug release property of mesoporous bioactive glasses (MBGs) and bioactive glasses (BGs) scaffolds. *Microporous Mesoporous Mater.* **118**, 176–182. (doi:10.1016/j.micromeso.2008.08.046)

92 Zhao, Y. F., Loo, S. C., Chen, Y. Z., Boey, F. Y. & Ma, J. 2008 *In situ* SAXRD study of sol–gel induced well-ordered mesoporous bioglasses for drug delivery. *J. Biomed. Mater. Res. A* **85A**, 1032–1042. (doi:10.1002/jbm.a.31545)

93 Lin, J., Fan, Y., Yang, P. P., Huang, S. S., Jiang, J. H. & Lian, H. Z. 2009 Luminescent and mesoporous europium-doped bioactive glasses (MBG) as a drug carrier. *J. Phys. Chem. C* **113**, 7826–7830. (doi:10.1021/jp900515x)

94 Fan, Y., Huang, S., Jiang, J., Li, G., Yang, P., Lian, H., Cheng, Z. & Lin, J. 2011 Luminescent, mesoporous, and bioactive europium-doped calcium silicate (MCS: Eu^{3+}) as a drug carrier. *J. Colloid Interface Sci.* **357**, 280–285. (doi:10.1016/j.jcis.2011.01.109)

95 Lopez-Noriega, A., Arcos, D. & Vallet-Regi, M. 2010 Functionalizing mesoporous bioglasses for long-term anti-osteoporotic drug delivery. *Chem. Eur. J.* **16**, 10 879–10 886. (doi:10.1002/chem.201000137)

96 Lin, H. M., Wang, W. K., Hsiung, P. A. & Shyu, S. G. 2010 Light-sensitive intelligent drug delivery systems of coumarin-modified mesoporous bioactive glass. *Acta Biomater.* **6**, 3256–3263. (doi:10.1016/j.actbio.2010.02.014)

97 Wu, C., Fan, W., Chang, J. & Xiao, Y. Submitted. Mesoporous bioactive glass scaffolds for efficient delivery of vascular endothelial growth factor.

98 Dai, C., Guo, H., Lu, J., Shi, J., Wei, J. & Liu, C. 2011 Osteogenic evaluation of calcium/magnesium-doped mesoporous silica scaffold with incorporation of rhBMP-2 by synchrotron radiation-based muCT. *Biomaterials* **32**, 8506–8517. (doi:10.1016/j.biomaterials.2011.07.090)

99 Wu, C., Fan, W., Gelinsky, M., Xiao, Y., Chang, J., Friis, T. & Cuniberti, G. 2011 *In situ* preparation and protein delivery of silicate–alginate composite microspheres with core-shell structure. *J. R. Soc. Interface* **8**, 1804–1814. (doi:10.1098/rsif.2011.0201)

100 Fan, W., Wu, C., Han, P., Zhou, Y. & Xiao, Y. Submitted. Porous Ca–Si-based nanospheres: a potential intra-canal disinfectant for infected canal treatment.

101 Deng, Y., Li, X. K. & Li, Q. 2009 Effect of pore size on the growth of hydroxyapatite from mesoporous $CaO–SiO_2$ substrate. *Ind. Eng. Chem. Res.* **48**, 8829–8836. (doi:10.1021/ie801796y)

102 Yu, C. Z., Wei, G. F., Yan, X. X., Yi, J., Zhao, L. Z., Zhou, L. & Wang, Y. H. 2011 Synthesis and *in-vitro* bioactivity of mesoporous bioactive glasses with tunable macropores. *Microporous Mesoporous Mater.* **143**, 157–165. (doi:10.1016/j.micromeso.2011.02.024)

103 Eden, M., Gunawidjaja, P. N., Lo, A. Y. H., Izquierdo-Barba, I., Garcia, A., Arcos, D., Stevensson, B., Grins, J. & Vallet-Regi, M. 2010 Biomimetic apatite mineralization mechanisms of mesoporous bioactive glasses as probed by multinuclear ^{31}P, ^{29}Si, ^{23}Na and ^{13}C solid-state NMR. *J. Phys. Chem. C* **114**, 19 345–19 356. (doi:10.1021/jp105408c)